Simulation of Arsenic *In Situ* Doping With Polysilicon CVD and Its Application to High Aspect Ratio Trenches

Clemens Heitzinger, Wolfgang Pyka, Naoki Tamaoki, Toshiro Takase, Toshimitsu Ohmine, and Siegfried Selberherr, *Fellow, IEEE*

***Abstract*—Filling high aspect ratio trenches is an essential manufacturing step for state of the art memory cells. Understanding and simulating the transport and surface processes enables to achieve voidless filling of deep trenches, to predict the resulting profiles, and thus to optimize the process parameters and the resulting memory cells.**

Experiments of arsenic doped polysilicon deposition show that under certain process conditions step coverages greater than unity can be achieved. We developed a new model for the simulation of arsenic doped polysilicon deposition, which takes into account surface coverage dependent sticking coefficients and surface coverage dependent arsenic incorporation and desorption rates. The additional introduction of Langmuir—Hinshelwood type time dependent surface coverage enabled the reproduction of the bottom up filling of the trenches in simulations. Additionally, the rigorous treatment of the time dependent surface coverage allows to trace the in situ doping of the deposited film.

The model presented was implemented and simulations were carried out for different process parameters. Very good agreement with experimental data was achieved with theoretically deduced parameters. Simulation results are shown and discussed for polysilicon deposition into 0.1 μm wide and 7 μm deep, high aspect ratio trenches.

***Index Terms*—Chemical vapor deposition (CVD), in situ doping, memory cells, topography.**

I. Introduction

VOIDLESS filling of deep trenches is a crucial process step in manufacturing state of the art memory cells. Our experiments of arsenic doped polysilicon deposition have shown that under certain process conditions step coverages greater than unity can be achieved. This means that the deposition rate at the bottom of the trench is higher than at the feature opening which leads to highly desired bottom up filling of the trench.

Understanding the mechanism of arsenic doped polysilicon deposition allows to optimize the filling of miniature trench structures. These features are, e.g., important for electrodes of memory capacitors and for contact structures, where the manufacturing processes have to be applicable to trenches of high aspect ratio. Thus the aims were to model the chemical vapor deposition (CVD) and surface reaction processes, to predict the resulting profiles from process parameters, to provide feedback for device design, and finally to optimize the manufacturing process with respect to manufacturing throughput.

In this paper, a new model for arsenic doped polysilicon is developed in order to trace the origin of the effect of bottom up filling and to facilitate its controlled application. The model takes into account surface coverage dependent sticking coefficients, surface coverage dependent arsenic incorporation and desorption rates, and Langmuir—Hinshelwood type time-dependent surface coverage. In addition the *in situ* doping of the deposited film is traced. The process considered is a high-pressure thermal CVD process, where no electric field effects occur, and the SiH_4 gas flow rate is about 1.2 slm, the AsH_3 flow rate is between 0 and 5 sccm, the N_2 flow rate about 40 slm, the total pressure is about 50 torr, and the temperature of the substrate is about 700 °C.

In Section II, the time and flux dependent surface reaction CVD model is presented. Furthermore, linking the reaction model and profile evolution is described along with simulation logic and the various other parts of the simulation program, namely surface extraction, meshing, and topography simulation. The arguments whether a diffusion or a radiosity approach should be used are discussed as well. Due to the general approach in the transport/reaction model description the implemented methodology has also been extended to other processes like the deposition of tungsten.

Simulation results from a 0.1-μm-wide and 7-μm-deep trench reflecting the experimental results are discussed in Section III, where the influence of different arsenic concentrations can be seen. Bottom up filling is reached in some cases. The arsenic incorporation rate was simulated as well. Results indicate that there are two different limitations for the deposition process. When the arsenic flow is low, the deposition process is concentration limited, since at the bottom of the trench no arsenic absorption layer is formed. In the second case, the supplied arsenic concentration is high enough to reach the bottom of the trench, and the diffusion process is only limited by the time allowed. This emphasizes the fact that the effects of surface layer formation are fundamental.

Manuscript received March 11, 2002; revised July 22, 2002. The work of C. Heitzinger was supported by the "Christian Doppler Forschungsgesellschaft," Vienna, Austria. This paper was recommended by Associate Editor W. Schoenmaker.

C. Heitzinger, W. Pyka, and S. Selberherr are with the Institute for Microelectronics, Technical University of Vienna, A-1040 Vienna, Austria (e-mail: heitzinger@iue.tuwien.ac.at).

N. Tamaoki, T. Takase, and T. Ohmine are with the Toshiba Corporate R&D Center, 212-8582 Kawasaki, Japan.

Digital Object Identifier 10.1109/TCAD.2002.807879

0278-0070/03$17.00 © 2003 IEEE

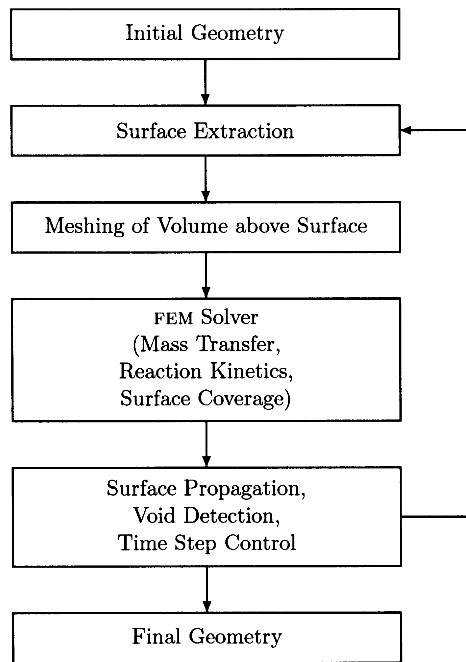

Fig. 1. Overview of the simulation logic.

II. Simulating Arsenic Doped Poly-Silicon Deposition

The simulator developed for CVD processes is a combination of specialized tools which are iteratively called. It was first described in detail in [1] and has been extended for the specific requirements for the simulation of time dependent processes like the deposition of arsenic doped polysilicon.

In general, a typical simulation flow is as follows (cf. Fig. 1). In the first step the surface of the initial geometry is extracted and used for generating a three-dimensional (3-D) mesh of the gas domain above the wafer surface. Secondly, a finite element solver operates on this unstructured tetrahedral mesh and solves the differential equations corresponding to mass transfer and reaction kinetics. The deposition rates obtained that way act as input to the topography simulator and are converted to a cellular representation. The topography simulator then propagates the surface, which leads to a new cellular topography.

This procedure is repeated for every time-step until the overall simulation time is completed. Certain parameters for the meshing tool and the continuum transport model are extracted from control files, which ensures automatic operations without further user interaction.

The accuracy of the simulation can be adjusted by the cell resolution. The drawback of higher resolutions are of course longer simulation times. Finally it is noted that the differences in molar mass, average molecular velocities, and diffusivities of the different gas species are treated rigorously after being read from control files.

A. Surface Extraction

In order to start the simulation flow, appropriate input for the meshing tool has to be prepared. The initial geometry is built with a solid modeling tool and the representation is based on the same cellular material representation used in the deposition simulator. Hence, the surface of the initial geometry as well as that of the geometries resulting after each time step have to be extracted into a triangular format that is suitable as input for the meshing tool.

The conversion is accomplished using a marching cube algorithm [2]. Its advantage is that it ensures that all triangle points are located in the center of the cell faces, which is necessary for an isomorphism between triangle points and surface cells. The only exception are points touching the horizontal bounding box. In this case the points are located at the edges of the cubes still permitting a one to one correspondence. After the initial triangulation, coplanar triangles are merged using a very small point to plane distance criterion according to [3]. Thus the following meshing and finite-element method (FEM) steps are highly efficient without losing any topography information.

B. Meshing

The meshing tool described in detail in [4] uses a modified advancing front algorithm to generate a three-dimensional unstructed tetrahedral mesh. Its input are the initial surface, which is given as a list of triangles and the size of the reactor region above the feature. Extra points within the region must be added in order to arrive at a suitable grid. The meshing tool can generate point clouds in surface normal style or as axis-aligned tensor product meshes.

When the surface has propagated after each time step, it is possible that some of the initially defined points of the ortho style point clouds are below the new surface. Since the advancing front algorithm propagates from the initial surface in a well-defined direction, those points are never reached by the front and are implicitly discarded. Therefore it is possible to use the same control file and the same initial point clouds for meshing the structures in different time steps, which is necessary for automating the simulation sequence.

C. Diffusion, Reaction Kinetics, and Surface Coverage

For the simulation of the chemical part of the model a program called Analytical Model Interface and General Object-oriented Solver (AMIGOS) [5] is used. It combines an interpreter for translating mathematical expressions into one-, two-, or three-dimensional discretized numerical representations and an input language for the formulation of the discretization scheme and the considered partial differential equations. The global equation system is assembled according to the discretization scheme, and the global system matrix is passed on to a numerical solver. The model definition interface of AMIGOS allows to flexibly choose the involved gas species and chemical reactions.

In order to solve the CVD model numerically, it was discretized using a finite element scheme. The CVD model is based on [6] and was extended in a number of ways: it was made time-dependent, the concept of surface coverages was added, and arbitrary chemical reactions can be specified by declaring the reactant types involved and the reaction equations. The governing principle of CVD determined by continuum transport is mass conservation which has to be respected in the time-dependent diffusion of gas species in the gas phase including homogeneous (volume) reactions and heterogeneous (surface) reactions with multiple species. In the high pressure regime

considered, diffusion is the predominant transport mechanism. At the top of the simulation domain constant concentration of the gas species is assumed and no flux across the side walls of the domain. The conditions at the top and at the side walls are handled as Dirichlet and Neumann boundary conditions, respectively. The diffusion and reaction equations contain the concentrations of all involved gas species, which are coupled by the stoichiometry of the chemical reactions. Consequently, transport of gas molecules from the plasma above the wafer into the trench competes with surface reactions which transform the reactants to a solid material forming the deposited layer.

In contrast to the reactive gas species, which are distributed in the whole reactor chamber and are treated in a volume model, the surface coverage is defined at the boundary of the simulation domain, which represents the surface of the feature. In the overall formulation of the model the surface coverage process is specified as a separate boundary model.

The assumptions for a steady-state surface coverage were valid and sufficient in prior work for different process chemistries [1], but do not hold for the chemical reaction system observed in the arsenic/silicon chemistry for polysilicon deposition. Due to the surface chemistry of this process, the assumptions leading to reaching a steady-state surface coverage fast are not valid and thus a rigorous time-dependent calculation of the surface coverage is required [7].

The transport of the reactants in the high-pressure regime (approximately 10 torr) is characterized by the diffusion equation

$$\frac{\partial c_i}{\partial t} = \nabla \cdot (D_i \nabla c_i) \tag{1}$$

where i stands for the three types of reactants, namely AsH_3, SiH_4, and SiH_2, c_i for their concentration, and D_i for their diffusivity.

The relevant gas species for the polysilicon deposition process are AsH_3, SiH_4, and SiH_2, where SiH_4 and SiH_2 react to form the polysilicon layer and AsH_3 is responsible for doping only and hence its concentration is lower than that of SiH_4 and SiH_2 by a factor of 10^3 or 10^4. AsH_3, SiH_4, and N_2 are introduced into the reactor. The principal reaction scheme is

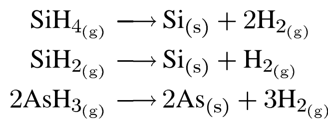

$$\mathrm{SiH}_{4(\mathrm{g})} \longrightarrow \mathrm{Si}_{(\mathrm{s})} + 2\mathrm{H}_{2(\mathrm{g})}$$
$$\mathrm{SiH}_{2(\mathrm{g})} \longrightarrow \mathrm{Si}_{(\mathrm{s})} + \mathrm{H}_{2(\mathrm{g})}$$
$$2\mathrm{AsH}_{3(\mathrm{g})} \longrightarrow 2\mathrm{As}_{(\mathrm{s})} + 3\mathrm{H}_{2(\mathrm{g})}$$

where only the main contributing reactions are considered in order to arrive at a reaction scheme without an abundance of unknown parameters. Furthermore, SiH_3 is not generated by thermal decomposition of SiH_4, since a high excitation energy would be needed. The reaction can be split into three stages, namely adsorption, the chemical reaction by itself and the desorption. The stages for silane are

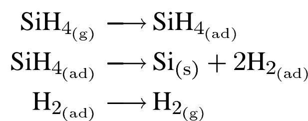

$$\mathrm{SiH}_{4(\mathrm{g})} \longrightarrow \mathrm{SiH}_{4(\mathrm{ad})}$$
$$\mathrm{SiH}_{4(\mathrm{ad})} \longrightarrow \mathrm{Si}_{(\mathrm{s})} + 2\mathrm{H}_{2(\mathrm{ad})}$$
$$\mathrm{H}_{2(\mathrm{ad})} \longrightarrow \mathrm{H}_{2(\mathrm{g})}$$

and analogously for SiH_2 and AsH_3, where (ad) denotes the adsorpted state in an arsenic inhibition layer [8].

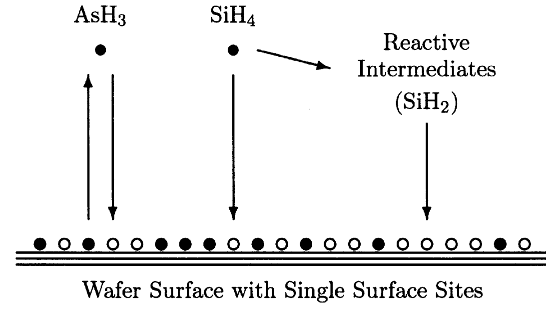

Fig. 2. Surface reaction and coverages.

The deposition velocity is governed by the adsorbed arsenic inhibition layer (cf. Fig. 2). The kinetics of the layer formation are given by

$$\frac{\partial C_s}{\partial t} = \eta_{\mathrm{AsH}_3} \Gamma_{\mathrm{AsH}_3} - k_s C_s - k_d C_s \tag{2}$$

where C_s is the arsenic density, and η_{AsH_3} and Γ_{AsH_3} denote arsenic sticking coefficient and flux, respectively. k_d is the rate constant of arsenic desorption from the protective layer and k_s the incorporation rate of arsenic from the layer into the deposited polysilicon film. The sticking coefficients for AsH_3 and SiH_4 are defined as

$$\eta_{\mathrm{AsH}_3} = \eta^0_{\mathrm{AsH}_3} \left(1 - \frac{C_s}{C_0}\right) \tag{3}$$

and

$$\eta_{\mathrm{SiH}_4} = \eta^0_{\mathrm{SiH}_4} \left(1 - \frac{C_s}{C_0}\right) \tag{4}$$

where $\eta^0_{\mathrm{AsH}_3}$ and $\eta^0_{\mathrm{SiH}_4}$ are the clean surface sticking probabilities and C_0 is the number of available surface sites per unit area for arsenic adsorption. In order to determine the sticking coefficient of SiH_2, the shape of polysilicon films on deep trench structures were examined in simulation results and scanning electron microscope (SEM) images. Values between 0.9 and 1 yielded the best match and thus a value of unity is used in the following. The final deposition rate has three contributions, namely polysilicon deposition from surface reactions of SiH_2 and SiH_4 at the unprotected surface and the incorporation of arsenic from the adsorption layer. Thus, the resulting deposition rate DR is given by

$$\mathrm{DR} = \eta_{\mathrm{SiH}_4} \Gamma_{\mathrm{SiH}_4} + \eta_{\mathrm{SiH}_2} \Gamma_{\mathrm{SiH}_2} + k_s C_s. \tag{5}$$

Again, η_i denote the sticking probabilities and Γ_i the corresponding fluxes. Since SiH_4 and SiH_2 are predominant, the AsH_3 flux can be safely neglected in the sum for the deposition rate. The coupling between gas concentrations c_i within the reactor space and the fluxes Γ_i toward the surface is given by the relation

$$\Gamma_i = \frac{\nu_i c_i}{4} \quad \text{with} \quad \nu_i = \sqrt{\frac{8kT}{\pi m_i}}. \tag{6}$$

Here, ν_i is the average molecular velocity of gas species i with a molar mass m_i.

The modeling equations described above result in a set of partial differential equations for the concentrations of the reactants

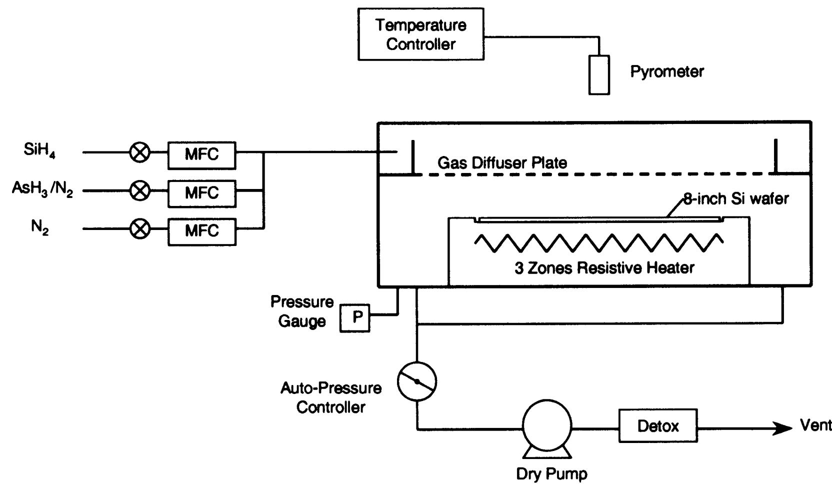

Fig. 3. The setup of the reactor used for the experiments.

and the surface coverage which is iteratively solved for the profile evolving with time. Most importantly, by tracing the actual surface coverage the model allows to monitor the arsenic incorporation into the polysilicon film and thus the *in situ* doping of the deposited layer.

The boundary condition for the model are the concentrations of the reactants on top of the simulation domain. Since the presence of arsenic determines the protective film formation and thus the behavior of the deposition rate, the most important influence is given by the AsH_3 partial pressure.

D. Diffusion Versus Radiosity

For the simulation of the transport of the particles above the wafer surface two main approaches are known, namely diffusion and radiosity. In the following, the arguments that contributed to the decision for using Knudsen diffusion instead of the radiosity approach are discussed.

The low sticking coefficients found for the particles moving above the wafer surface suggest a rather diffuse transport of the particles within the trench as opposed to the directed fluxes given in ballistic transport determined processes with sticking coefficients closer to unity.

Judging from SEM pictures of the trench (cf. Fig. 4) it can be concluded that the profile at the trench mouth is uniform, i.e., the thickness on top of the wafer, where no reflections can occur, is the same as on the sidewall at the trench mouth. This is contradictory to ballistic transport models which show a strong dependence of the film profile on the orientation of the exposed surface.

Knudsen diffusion has been applied successfully to tungsten and TiN deposition processes in the same pressure and temperature regime, where the diffusion approach together with a different set of reaction equations has shown an excellent agreement between the simulated and experimentally observed overhang structures.

Even without calibration or fitting parameters the simulation results clearly represent the experimentally observed bottom-up filling and the step coverage greater unity occurring at AsH_3 flow rates of about 0.3 sccm.

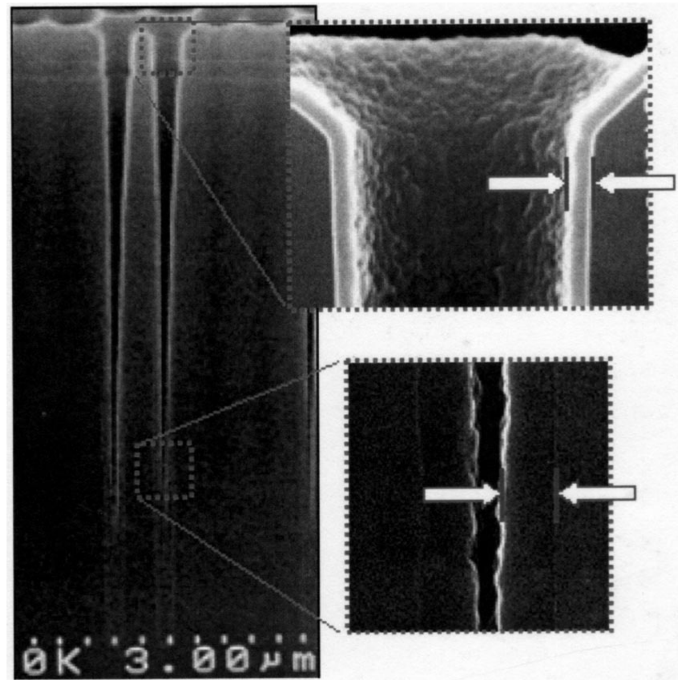

Fig. 4. SEM (scanning electron microscope) images of 7-μm-deep trenches.

Finally, since time dependence and spatial transport can be calculated simultaneously, the performance of the model drastically improves. Furthermore, conversions from cell to triangle format and orientation inaccuracies inevitable in an approach coupling radiosity and surface reactions are avoided.

E. Topography Simulation

Having calculated the deposition rates as described above, the wafer surface has to propagated. To that end a cell based topography simulator is used, which was first presented in [9] and has been extended and improved as described in [1] and [10] since. The geometry is represented by an array of cubic cells, which have unique material indices. Zero indicates that the cell is outside the wafer, whereas positive integer numbers indicate the material of the cell, if it lies within the wafer. When propagating the surface, a structuring element whose size depends

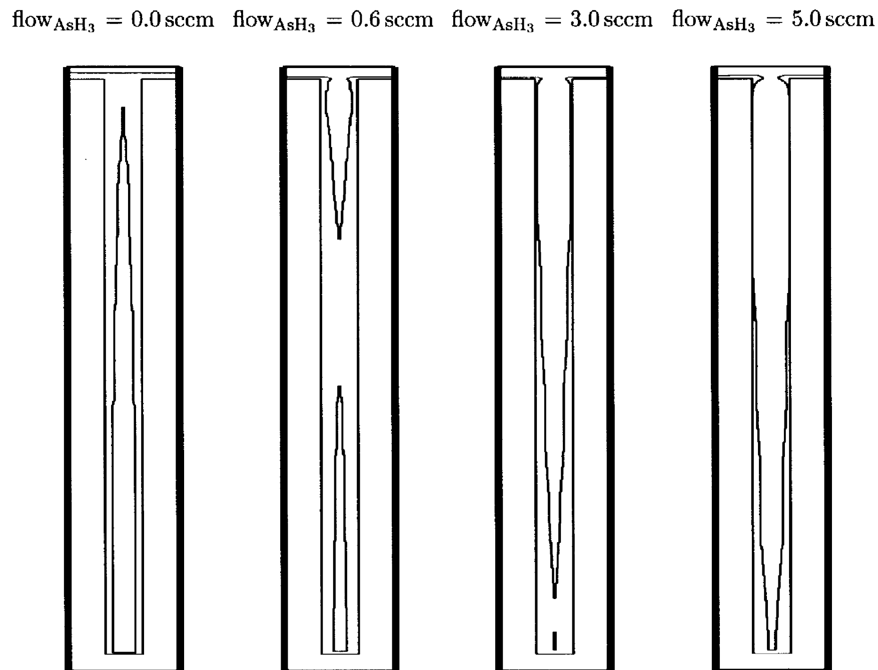

Fig. 5. Profile evolution of arsenic doped polysilicon deposition with AsH_3 flow increasing from left to right. Note the distorted width/height ratio of the figures, originally it is 0.3–7.35 μm.

on the local deposition rate is moved along the surface, and all vacuum cells hit by the element are switched to the index of the deposited material.

The deposition rates for the high-pressure model are read from the AMIGOS result file. This file contains the triangles generated by the surface extraction algorithm from Section II-A and additional rate values for each triangle point. These triangle points positioned in the center of the cell faces are assigned to the corresponding surface cells. In order to ensure a smooth and continuous surface evolution, it is necessary to apply structuring elements at all surface cells, which is accomplished by linear interpolation of the deposition rates within the triangles.

Time step control plays an important role, especially when the process conditions lead to the formation of voids. Depending on the interaction between diffusion velocity and reaction rates, depletion of gas species at the bottom of the feature is observed, which consequently leads to strong variations of the local deposition rates, to the characteristic overhang structures, and finally to the formation of voids. Within the cellular material representation, a region of vacuum cells not connected with the gas domain above the surface can easily be detected and used for controlling void closure. To avoid underestimating the size of such a void by choosing a too large time step when the void is closed, the topography simulator checks for voids and reduces the time step until it observes that the void is closed. In general, a constant time step is used.

III. Simulation Results for High Aspect Ratio Trenches

Experiments were carried out for 0.1-μm-wide and 7-μm-deep trenches in a custom-built single-wafer type reactor as shown in Fig. 3. SEM images of the experiments are depicted in Fig. 4. The simulation results for a trench of the same dimensions in Fig. 5 demonstrate the effect of increasing AsH_3 partial pressure (from left to right) which is controlled by the AsH_3 flow given in sccm (standard cubic centimeter per minute). Note the distorted width/height ratio of the figures, which originally is 0.3 μm to 7.35 μm. When no or little AsH_3 is present (left) no inhibition of the surface reaction is given and the usual step coverage smaller than unity and severe void formation are observed. With addition of AsH_3 an inhibiting layer is formed at the trench opening, lowering the deposition rate but shifting the effect of void formation to a lower region in the trench. With an even higher addition of AsH_3 the deposition is retarded in the complete trench, but in the upper part with the higher arsenic concentration more than in the lower part. In this case bottom-up filling is reached.

Still increasing the AsH_3 partial pressure amplifies this effect, but the possibility of the formation of a small overhang at the trench opening is given by SiH_2 contributions, which become the predominant fraction of the deposition rate under these process conditions. Note that increasing the AsH_3 partial pressure, and thus the formation of the resulting inhibition layer, reduces the deposition rate. Therefore, longer deposition times are necessary to obtain a film thickness of 100 nm, to which the simulations are scaled. The deposition times range from 15 to 180 s.

In Figs. 6 – 9, the arsenic incorporation rates corresponding to the profiles from Fig. 5 are shown. It is proportional to the surface coverage prevailing in the different trench regions and represents a measure for the *in situ* doping of the deposited film. The figures also suggest that for low AsH_3 flows the surface coverage is concentration limited, whereas it is time limited for higher flows. Concentration limited (the two figures on the left hand side) means that the available arsenic is completely consumed by the layer formation in the upper region of the trench.

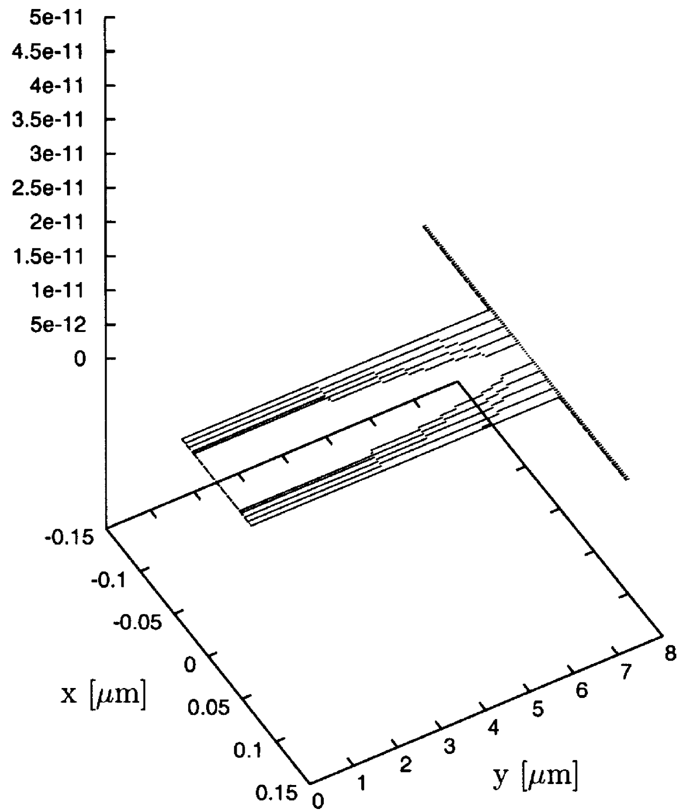

Fig. 6. Arsenic incorporation rates corresponding to the profile for $\mathrm{flow}_{\mathrm{AsH_3}} = 0.0$ sccm from Fig. 5. The rates are shown for 1.93, 3.85, 5.78, 7.69, and 9.60 s after the start of the simulation.

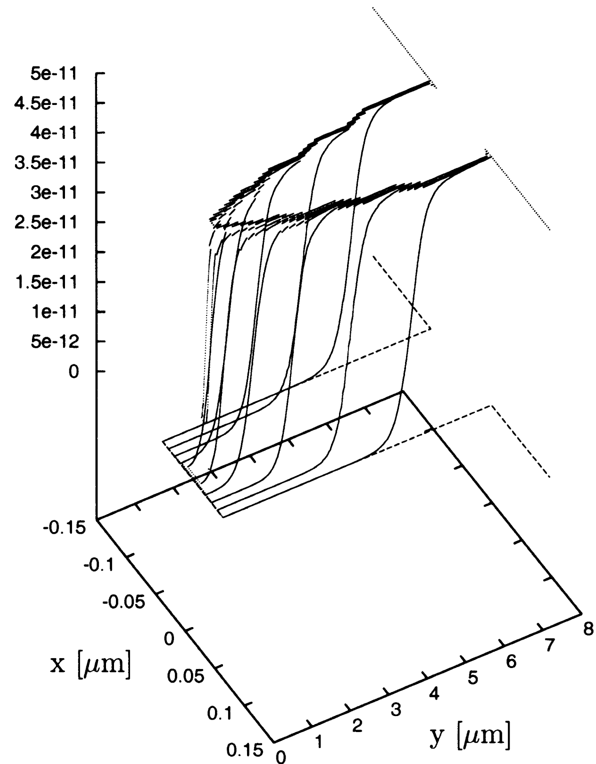

Fig. 8. Arsenic incorporation rates corresponding to the profile for $\mathrm{flow}_{\mathrm{AsH_3}} = 3.0$ sccm from Fig. 5. The rates are shown for 2.78, 5.78, 8.81, 11.58, 13.63, 16.37, 54.25, 92.01, and 99.66 s after the start of the simulation.

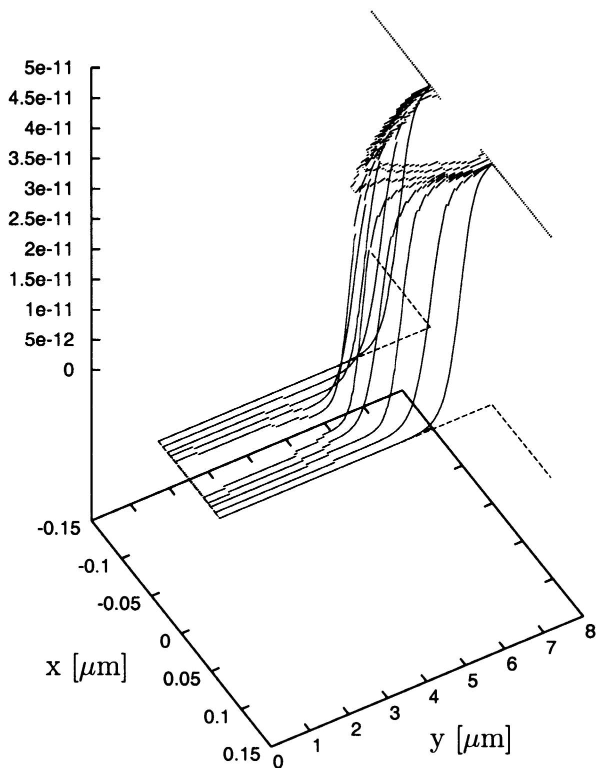

Fig. 7. Arsenic incorporation rates corresponding to the profile for $\mathrm{flow}_{\mathrm{AsH_3}} = 0.6$ sccm from Fig. 5. The rates are shown for 2.53, 5.26, 8.30, 11.55, 15.04, 30.58, 52.49, and 74.75 s after the start of the simulation.

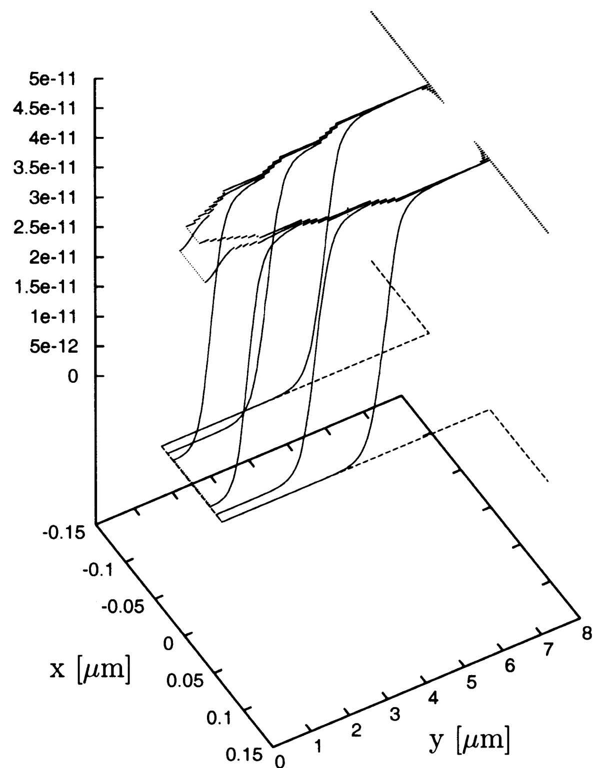

Fig. 9. Arsenic incorporation rates corresponding to the profile for $\mathrm{flow}_{\mathrm{AsH_3}} = 5.0$ sccm from Fig. 5. The rates are shown for 2.86, 5.85, 8.48, 23.92, 71.92, 112.14, 149.84, and 186.75 s after the start of the simulation. Some of the lines at the end of the simulation overlap.

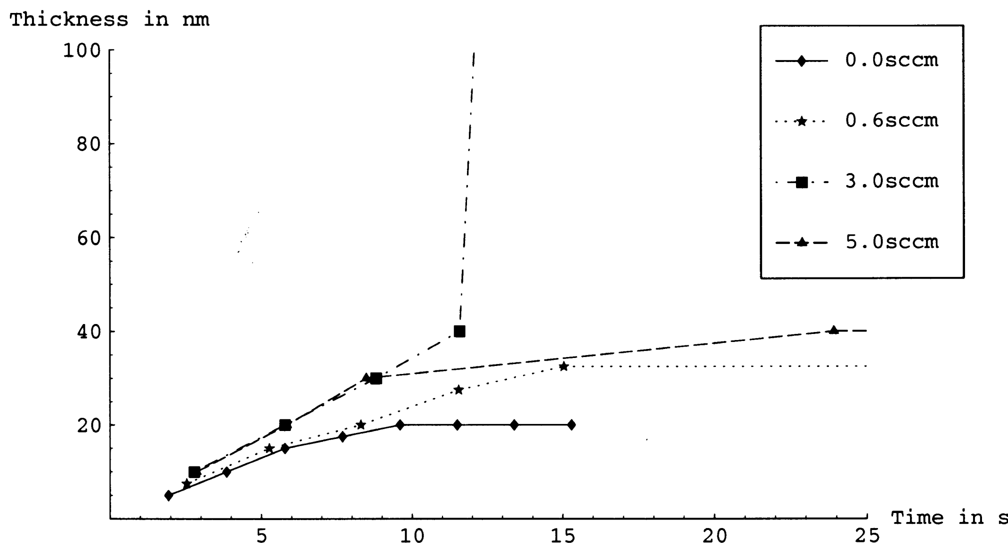

Fig. 10. The thickness (nm) of the deposited layer at the middle of the trench bottom depending on time (s). The four curves correspond to the four different AsH_3 flow rates (cf. Fig. 5) of 0.0, 0.6, 3.0, and 5.0 sccm.

Even for longer times no significant surface coverage can be observed at the bottom of the trench. Time limitation for higher flows (the two figures on the right hand side) means that enough arsenic is present for covering the complete trench, but it takes some time until the arsenic has diffused into the lower regions of the trench.

Finally, in Fig. 10, the time evolution of the thicknesses of the deposited layers at the middle of the trench bottom are compared for the four different AsH_3 flow rates. The four curves correspond to the four different AsH_3 flow rates (cf. Fig. 5). The thicknesses for flow rates of 0.0 and 0.6 sccm remain constant after voids have formed. The thickness for a flow rate of 3.0 sccm raises abruptly when the sidewalls meet. The thickness for 5.0 sccm raises only slowly because of the strong inhibition caused by the high AsH_3 flow.

The key to arriving at advantageous process conditions is leaving behind the concentration limited case and to just reach the time limited case. But going beyond a certain limit and too far into the second regime, the deposition rate decreases significantly, when the arsenic concentration is too high.

The simulation results from above clearly show that the formation of a surface coverage layer has the strongest influence on the profile evolution. The surface layer formation is determined by the amount of arsenic reaching the surface, which in the presented model is determined by three parameters, namely the concentration of AsH_3 on top of the simulation domain (corresponding to a Dirichlet boundary condition), the height of the simulation domain and the transport velocity, given by the diffusivity. Determining these parameters is crucial for the simulation.

In addition, the simulation domain can optionally be split into two regions. The two regions are the inner part of the trench and a boundary layer toward the reaction chamber outside the trench. The Knudsen diffusivity is different within the trench, where the characteristic diffusion length is determined by the trench diameter, and outside the trench, where the diffusivities are higher. This two regions approach allows for a more realistic approach to the transport phenomena and for an easier calibration of the parameters.

The simulations shown are intended to demonstrate the fundamental effects of surface layer formation on profile evolution, and therefore, assume only a very thin boundary layer. Thus the ideal AsH_3 flow obtained from the simulations slightly differs from the experimentally observed one. This difference can be further reduced by an accurate calibration of the transport parameters from the reactor scale (AsH_3 inlet gas flow) to the feature scale concentrations in the boundary layer and close to the trench surface.

Finally, it is noted that the CPU time consumed for these simulations is in the range of 10 to 30 min using a Pentium-III-based workstation.

IV. Conclusion

We have shown that by introducing Langmuir—Hinshelwood type time-dependent surface coverages into CVD modeling it is possible to simulate the bottom-up filling behavior of arsenic doped polysilicon trench filling. Furthermore, the rigorous treatment of the time-dependent surface coverage allows for the monitoring of the *in situ* doping of the deposited film, which is important for the characterization of the electrical properties of the deposited polysilicon film.

Bottom-up filling can be achieved by increasing the AsH_3 fraction in the process gas. On the other hand an increase in the AsH_3 fraction also reduces the overall deposition velocity of the process. In order to obtain a satisfactory profile evolution, the right balance between decreasing the probability of void formation and reducing the deposition velocity with respect to manufacturing throughput has to be found.

Concerning the industrial practicability, the deposition time is increased from about 15 s to about 1 min in order to suppress void-formation. But the cost of the whole industrial process is determined by many factors, not only by the deposition time of a single step. The benefit of voidless filling of deep trenches,

which cannot be achieved by other means, is worth the increased deposition time in the industrial application. Nevertheless, an acceptable deposition rate of about 1000 Å/min was achieved in practice.

Summarizing, having extracted the transport and reaction parameter, the simulation can be applied to test the influence of different sidewall slope angles on void formation and to finding the optimum AsH_3 flow for best deposition results. In order to obtain a satisfactory profile evolution without void formation, the right balance between the observed effects and the reduction in deposition velocity for higher AsH_3 flows has to be found.

References

[1] W. Pyka, P. Fleischmann, B. Haindl, and S. Selberherr, "Three-dimensional simulation of HPCVD—linking continuum transport and reaction kinetics with topography simulation," *IEEE Trans. Computer-Aided Design*, vol. 18, pp. 1741–1749, Dec. 1999.

[2] W. Lorenson and H. Cline, "Marching cubes: a high resolution 3D surface construction algorithm," *Comput. Graph.*, vol. 21, no. 4, pp. 163–169, 1987.

[3] W. Schroeder, J. Zarge, and W. Lorenson, "Decimation of triangle meshes," *Comput. Graphics*, vol. 26, no. 2, pp. 65–70, 1992.

[4] P. Fleischmann, W. Pyka, and S. Selberherr, "Mesh generation for application in technology CAD," *IEICE Trans. Electron.*, vol. E82-C, no. 6, pp. 937–947, 1999.

[5] M. Radi, E. Leitner, and S. Selberherr. (1999) AMIGOs: analytical model interface & general object-oriented solver. *IEEE J. Technology Computer–Aided Design* [Online] http://www.ieee.org/products/online/journal/tcad/accepted/radi-feb99/

[6] H. Liao and T. Cale, "Low-knudsen-number transport and deposition," *J. Vac. Sci. Technol. A*, vol. 12, no. 4, pp. 1020–1026, 1994.

[7] W. Pyka, C. Heitzinger, N. Tamaoki, T. Takase, T. Ohmine, and S. Selberherr, "Monitoring arsenic in-situ doping with advanced models for poly-silicon CVD," in *Proc. Simulation Semiconductor Process. Devices*, Athens, Greece, Sept. 2001, pp. 124–127.

[8] G. Schumicki and P. Seegebrecht, *Prozeßtechnologie*. Berlin, Germany: Springer, 1991.

[9] E. Strasser and S. Selberherr, "Algorithms and models for cellular based topography simulation," *IEEE Trans. Computer-Aided Design*, vol. 14, pp. 1104–1114, Sept. 1995.

[10] W. Pyka, R. Martins, and S. Selberherr, "Efficient algorithms for three-dimensional etching and deposition simulation," in *Proc. Simulation Semiconductor Process. Devices*, K. D. Meyer and S. Biesemans, Eds., Leuven, Belgium, Sept. 1998, pp. 16–19.

Clemens Heitzinger was born in Linz, Austria, in 1974. After the compulsory military service he studied mathematics at the University of Technology, Vienna, Austria, where he received the degree of Diplom-Ingenieur (with honors), in 1999, and the doctoral degree in technical sciences (with honors) from Technical University of Vienna, Vienna, Austria, in 2002.

In 2000, he joined the Institute for Microelectronics, Technical University of Vienna, Vienna, Austria. From March to May 2001, he held a position as Visiting Researcher at the Sony Atsugi Technology Center, Tokyo, Japan. His scientific interests include applied mathematics for the simulation of semiconductor processes and devices.

Wolfgang Pyka was born in Innsbruck, Austria, in 1970. He received the Diplom-Ingenieur in materials science from the Montanuniversität Leoben in 1996 and then joined the doctoral programme of the Institute for Microelectronics, Technical University of Vienna, Vienna, Austria, from where he received the doctoral degree in the technical sciences in 2000.

In summer 1998 and 1999, he was a visiting researcher at LSI Logic, Milpitas, CA. His work is focused on simulation and modeling of etching and deposition processes and on algorithms for topographic simulation and 3-D geometry generation.

Naoki Tamaoki was born in Kawasaki, Japan, in 1966. He received the M.Sc. degree in physics from Sophia University, Tokyo, Japan, in 1992.

He joined Toshiba in 1992 and is currently research scientist at the Corporate Research and Development Center, Toshiba Corporation, Kawasaki, Japan. His research interests are primarily in thermal CVD, chemical etching and process modeling.

Toshiro Takase was born in Tokyo, Japan, in 1967. He received the M.S. degree from the University of Tokyo, Tokyo, Japan, in 1992.

He worked as an exchange student in the Photon Factory, National Laboratory for High Energy Physics (KEK), Japan from 1992 to 1994. He joined Toshiba in 1994 and is currently research scientist at the Corporate Research and Development Center, Toshiba Corporation, Kawasaki, Japan. His research interests are primarily in TCAD process simulation and modeling.

Toshimitsu Ohmine was born in Tokyo, Japan, in 1949. He studied chemical engineering at the Tokyo Institute of Technology, where he received the degree of Master of Engineering in 1975.

He joined Toshiba, Kawasaki, Japan, in 1975, where he, finally as a chief research scientist, carried out research on semiconductor processes until 2002, when he retired. His last work includes TCAD process simulation and physical modeling.

Siegfried Selberherr (M'79–SM'84–F'93) was born in Klosterneuburg, Austria, in 1955. He received the degree of Diplom-Ingenieur in electrical engineering and the doctoral degree in technical sciences from the Technical University of Vienna, Vienna, Austria,in 1978 and 1981, respectively.

He has been holding the venia docendi on Computer-Aided Design since 1984. Since 1988, he has been the head of the Institut für Mikroelektronik, and since 1999, he has been dean of the Fakultät für Elektrotechnik. His current topics are modeling and simulation of problems for microelectronics engineering.